Unravelling CO_2 transfer through cork stoppers for Champagne and sparkling wines

Kevin Crouvisier Urion[a,b], *Jean-Pierre Bellat*[a], *Gérard Liger-Belair*[c], *Régis D. Gougeon*[b,d], *and Thomas Karbowiak*[b,*]

[a]*Univ. Bourgogne Franche-Comté, ICB UMR 6303 CNRS, 9 avenue Alain Savary, B.P. 47870, 21078 Dijon, France*

[b]*Univ. Bourgogne Franche-Comté, Agrosup Dijon, UMR PAM A 02.102, 1 Esplanade Erasme, 21000 Dijon, France*

c Univ. Reims Champagne-Ardenne, Equipe Effervescence, Champagne et Applications (GSMA), UMR CNRS 7331, BP 1039, 51687 Reims Cedex 2, France

[d]*Univ. Bourgogne Franche-Comté, Inst. Univ. Vigne & Vin, 1 Rue Claude Ladrey, F-21078 Dijon, France*

Corresponding Author*

Professor Thomas Karbowiak

thomas.karbowiak@agrosupdijon.fr

Phone: +33 (0)3 80 77 23 88

Abstract

The diffusion of CO_2 through macro- and micro-agglomerated cork stoppers for sparkling wine was studied by a manometric technique. The effective diffusion coefficients for each part of the stopper (cork body, cork disc and adhesives) were determined for the first time. The results show that a small particle size along with a high adhesive content and level of compression favor the gas barrier properties of the cork stopper. Although the cork discs placed at one end of the stopper present no resistance to gas transfer, the adhesive film between them constitutes a high barrier to gas transfer. The mechanism that controls the gas transfer is the solution-diffusion process through the polymeric chains of the adhesive. Although the aging of the cork stopper and the gas transfer at the glass/stopper interface were not considered, results clearly showed that the cork stoppers studied were capable of maintaining a CO_2 concentration in the bottle that is sufficient for conserving a good effervescence of sparkling wines over several years.

Keyword: Agglomerated cork stopper, CO_2, diffusion, gas transfer

1. Introduction

Cork has been used for centuries as corking material for wine conservation, from the amphora to the glass bottle. Agglomerated cork stoppers, made of cork particles with adhesives, were developed at the beginning of the twentieth century[1], first for sparkling wines and then extended to still wines. Cork particles, calibrated as a function of their mean diameter, form the "body" of the sparkling wine stopper. Since the 1970s, the agglomeration of cork particles has been made with polyurethane (PU) adhesives[2] to replace casein glue, which was initially used. In addition, two cork discs are usually glued with an aqueous dispersion of PU on one end of this agglomerated body, thus forming the "mirroir", which is in contact with the wine (Fig. 1).

Such agglomerated cork stoppers are used for the conservation of sparkling wines, such as Champagne, Crémant, Cava, Prosecco, Sekt, but also ciders and beers. Stoppers are highly compressed in the bottleneck. In the case of Champagne wine, this leads to a reduction in diameter of 45 % (from 31 mm to 17.5 mm diameter)[3], which corresponds to a reduction of 70 % in volume. After alcoholic fermentation has produced a still "base wine", these sparkling beverages are obtained either from a second fermentation step (using mainly *Saccharomyces cerevisiae*) or from carbonation, both leading to the presence of CO_2 dissolved in the liquid phase. Dissolved CO_2 concentrations range from 5 $g.L^{-1}$ for ciders and beers[4] up to 12 $g.L^{-1}$ for carbonated and sparkling wines[5]. When these beverages are bottled, the thermodynamic equilibrium between the gas-phase and dissolved CO_2 causes a partial pressure of gas-phase CO_2 in the headspace ranging from about 0.3 to 0.6 MPa (considering a Henry's constant value of 4.4×10^{-4} $mol.m^{-3}.Pa^{-1}$ at 12 °C)[6]. Consequently, the high partial pressure gradient of gas-phase CO_2 between the inside and outside of the bottle leads to a CO_2 transfer through the stopper, which causes a progressive loss of dissolved CO_2 from the liquid phase. Nevertheless, below a partial pressure close to 0.13 MPa

in the headspace (at 12 °C)[6], corresponding to a critical concentration of dissolved CO_2 close to 2.5 $g.L^{-1}$, a sparkling wine becomes thermodynamically unable to promote effervescence. The precise knowledge of the permeability of a cork stopper with regard to gas-phase CO_2 becomes therefore crucial to understand how a bottle of sparkling wine progressively loses its dissolved CO_2 content, and therefore its bubbling potential.

The first study dealing with gas transfer through the cork stopper was conducted in the mid-1990s[7]. Since then, numerous studies have investigated the gas transfer through wine stoppers, in particular to the O_2 transfer, because of its impact on wine oxidation[8]. Several techniques have been developed to study gas transfer through stoppers, such as coulometric detection, manometric devices, chemiluminescence, SO_2 titration, and colorimetric method. Synthetic stoppers exhibit the highest oxygen transfer rate (from 10^{-6} to 10^{-4} mmol $O_2.m^{-2}.s^{-1}$), followed by natural cork (10^{-7} to 10^{-3} mmol $O_2.m^{-2}.s^{-1}$), screwcaps (10^{-8} to 10^{-4} mmol $O_2.m^{-2}.s^{-1}$) and technical stoppers (10^{-7} to 10^{-5} mmol $O_2.m^{-2}.s^{-1}$), at room temperature for an oxygen partial pressure gradient of 0.21 MPa[9]. However, only a few studies have addressed the issue of CO_2 transfer[10-13], and only two deal with sparkling wine stoppers[5, 6]. Based on the CO_2 concentration decrease in sparkling wine bottles and using modeling (based on Henry's and Fick's laws), the effective CO_2 diffusion coefficient has recently been estimated to be between 5 x 10^{-11} and 3 x 10^{-10} $m^2.s^{-1}$[5, 6]. However, to date, there has been no direct and accurate experimental measurement of the effective diffusion coefficient of CO_2 through composite materials such as agglomerated stoppers, in which each part constitutes an individual resistance to gas transfer.

Sparkling wine stoppers, made of a body of agglomerated cork particles with two cork discs fixed on one end with two films of adhesive can be considered as an equivalent system composed of five resistances to mass transfer connected in series (Fig. 2). This macroscopic view could obviously be more detailed depending on the scale that is considered. Cork itself

85 is an alveolar material composed of empty closed cells of about 30 µm characteristic
86 dimension with a cell wall around 1 µm thickness. It also contains macroscopic pores called
87 lenticels with a diameter in the millimeter scale. In the case of agglomerated cork stopper,
88 cork particles are surrounded by polyurethane. There is also an intergranular porosity between
89 these particles, which may be either opened or closed. Therefore, it is essential to identify the
90 limiting step for gas transfer and the associated diffusion mechanism. Three mass transfer
91 mechanisms can occur in such a material[9]: (i) the molecules move in macropores according
92 to Darcy's law, when the mean free path of the diffusing molecule is lower than the pore
93 diameter; (ii) the molecules diffuse in mesopores following a Knudsen's regime, when the
94 mean free path of the diffusing molecule is larger than the pore diameter; and (iii) the
95 molecules move by jumping from one sorption site to another one in a phenomenon called
96 surface diffusion or solution-diffusion process in the case of polymeric networks [14].

97 The objective of this study was to measure the effective diffusion coefficient of gas-phase
98 CO_2 through an agglomerated cork stopper and then to identify the limiting step to gas
99 transfer depending on the composite material structure. To that purpose, it was necessary to
100 experimentally determine the gas transfer through each part of the sparkling wine stopper.
101 Furthermore, the different parameters that can control the gas transfer, such as the cork
102 particle size, the adhesive content, the presence of cork discs, and the effect of the
103 compression were investigated. The results of CO_2 transfer through sparkling wine stoppers
104 are critically analyzed in order to better understand the gas barrier properties of stoppers and
105 to estimate their impact on the shelf life of sparkling wines.

106

2. Materials and methods

2.1. Material: Cork stoppers

Agglomerated cork stoppers were supplied by the Relvas (Mozelos, Portugal) and Prats & Bonany (Reims, France) companies. Two types of stoppers were studied: stoppers composed of a macro-agglomerated body with two cork discs at one end (referred to as MA2D) and stoppers composed only of a micro-agglomerated cork body (referred to as MI). Two cork particle size distributions, determined according to the NP ISO 2031:2015 standard, were used to formulate macro-agglomerated (2.5-8 mm diameter) and micro-agglomerated (0.5-2.8 mm diameter) stoppers. An aromatic glue, composed of toluene diisocyanate (TDI) isomers (2,6-TDI and 2,4-TDI), was used at mass ratios (w_{glue}/w_{cork}) of 8 % and 15 % for macro-agglomerated and at 20 % and 25 % for micro-agglomerated stoppers. Agglomerated cork bodies were obtained after polymerization at 120 °C for 45-65 min using an industrial scale processing, based on individual molding. Two cork discs (6 mm thick) were glued at one end of the agglomerated cork body with an aqueous dispersion of PU. They are referred to as “aromatic adhesive for cork body” and “cork disc adhesive”, respectively, in the present paper. The resulting stoppers were then sanded down and chamfered to obtain the final cork stopper for sparkling wine. The diameter was reduced to 30 mm to meet the requirements of the bottling machine (TDD Grillat, BM 800).

2.2. Gas transfer measurement

The gas transfer through the samples was measured using a homemade manometric device. The equipment and the procedure used to determine the effective diffusion coefficient were previously detailed in Chanut *et al.* (2020)[15] . It is based on the pressure measurement in two compartments separated by the sample. For the present work, the initial pressure was fixed at 0.6 MPa of pure CO_2 in the first compartment, corresponding to the pressure of CO_2

inside a Champagne wine bottle at the end of the fermentation step. The second compartment of the device was maintained under dynamic primary vacuum (0.1 hPa). The pressure drop in the first compartment, due to CO_2 transfer through the sample, was recorded over time. The temperature was kept constant at 25 °C. The accuracy of the pressure sensor was 0.01 MPa. As the calculation of the effective diffusion coefficient requires the knowledge of the solubility of CO_2 in the materials, the sorption isotherms of CO_2 on the agglomerated cork and on the adhesives were previously determined from 0 to 5 MPa, at 25 °C, using a magnetic suspension balance (Rubotherm GmbH). Rectangular samples (~ 150 mm^3) were first outgassed at 25 °C under primary vacuum until mass equilibrium. The gas pressure in the balance was then increased step-by-step (once mass equilibrium was reached for each pressure step). A specific module allowed measuring the gas phase density in order to take into account the buoyancy effect. For each sample, the sorption and desorption isotherms of CO_2 were determined, as displayed in Fig. 3, and allows to determine the partition coefficient ψ, defined as the ratio between the concentration of CO_2 sorbed on the material ($mol.m^{-3}$) and the concentration of CO_2 in the gas phase in contact with the film ($mol.m^{-3}$) at equilibrium.

The different geometries used to determine the effective diffusion coefficient of CO_2 according to the sample are summarized in Table 1. To reduce the experimental time, gas transfer was not measured on full-length stoppers, but on reduced-thickness samples. To determine the gas transfer on a full-length stopper, an extrapolation model was applied, following the procedure detailed in Lagorce-Tachon *et al.* (2016) and Chanut *et al* (2020)[15, 16], as shown in Fig. 4 for a macro-agglomerated cork body containing 8 % aromatic adhesive. CO_2 transfer measurements were carried out on agglomerated corks, both compressed and non-compressed, on the different adhesive films composing the stopper (~700 µm thickness films obtained by polymerization at 20 °C) and on the cork discs. The compressed samples were obtained using a corking machine (TDD Grillat, BM 800) equipped

158 with a special homemade device, which allowed insertion of the cork slice in a sample holder
159 of 17.0 (± 0.5) mm diameter (corresponding to a Champagne bottleneck).

160 2.3. Helium pycnometry

161 The porosity of the samples has been measured by helium pycnometry with a
162 homemade manometric device. Prior to the measurement, the sample was outgassed under
163 primary vacuum at room temperature. A cork body sample of known apparent volume V_{app}
164 (measured with a caliper) was introduced in the helium pycnometer and the real volume of the
165 sample V_s was determined from pressure measurements. The porous fraction V_p is defined as
166 the ratio of the volume accessible to helium over the apparent volume, according to the
167 following equation:

168 $$V_p(\%\, V/V) = \left(\frac{V_{app} - V_s}{V_{app}}\right) \times 100 \qquad (1)$$

169 Helium pycnometry was performed at 25 °C on 10 macro- and micro-agglomerated cork
170 bodies (with an apparent diameter of 3.00 ± 0.01 cm and a length of 4.80 ± 0.02 cm, which
171 corresponds to an apparent volume of 34.4 ± 0.3 cm^3.

172 2.4. Scanning electron microscopy (SEM)
173
174 Agglomerated cork stoppers for sparkling wine were observed by SEM using a Jeol JSM
175 7600F instrument. Prior to imaging, samples were cut with a razor blade and coated with 15-
176 20 nm carbon. A vacuum of 9 x 10^{-6} Pa was applied with an accelerating voltage of 15 kV.

177

3. Results and discussion

3.1. Effect of particle size and adhesive concentration of the cork body

Fig. 5 displays the extrapolated distribution for CO_2 effective diffusion coefficients (D) obtained for non-compressed macro- and micro-agglomerated cork bodies with two different amounts of aromatic adhesive. The mean values of effective diffusion coefficients are also indicated in Table 2. It is noteworthy that the distribution of effective diffusion coefficient values is very large. This is due to the heterogeneity of the porosity of such agglomerated materials, which are composed of cork particles having various sizes and geometries. Both the increase in adhesive concentration and the reduction in the cork particle size lead to a decrease in the mean value of D. A decrease by a factor of 3 (from 3×10^{-5} to 9×10^{-6} $m^2.s^{-1}$) is observed for the macro-agglomerated cork body with an increase in the adhesive content from 8 % to 15 %, and by a factor of 4 (from 8×10^{-8} to 2×10^{-8} $m^2.s^{-1}$) when the adhesive content increases from 20 % to 25 % for the micro-agglomerated cork body (Table 2). Regarding the cork particle size, the reduction from macro (2.5-8 mm) to micro (0.5-2.8 mm) leads to a decrease in the CO_2 effective diffusion coefficient by a factor of 375 (from 3×10^{-5} to 8×10^{-8} $m^2.s^{-1}$). This clearly highlights that within the investigated range, particle size is a predominant factor in the reduction of effective diffusion coefficient compared with the increase in adhesive concentration. Nevertheless, the effect of these two factors cannot be fully separated, the micro-agglomerated cork formulation requiring a higher adhesive concentration to obtain an agglomerated body suitable for stopper application.

The decrease in the CO_2 effective diffusion coefficient in agglomerated cork with increasing adhesive concentration may be due to the barrier property of the adhesive used for agglomeration. The aromatic PU glue used in sparkling wine stoppers has an average CO_2 effective diffusion coefficient value of 8×10^{-11} $m^2.s^{-1}$ (Table 2). This value is in agreement

with those found in the literature. Depending on the nature of the monomer used and its content, there is a variation in D values from 7 x 10^{-11} to 1 x 10^{-10} $m^2.s^{-1}$[17].

Our results show that the higher the adhesive content, the better the CO_2 barrier property. This effect is probably due to the presence of a continuous adhesive film surrounding the cork particles, which is favored when the particles are small. In addition, the intergranular porosity decreases in the micro-agglomerated cork body with smaller particle size. Moreover, in the latter case, the cork particles are smaller and more spherical in shape than those used for the macro-agglomerated cork. This modification in size and shape induces a reduced intergranular porosity[18, 19]. For a deeper understanding of the difference between the macro- and micro-agglomerated cork bodies, it is thus necessary to measure the intergranular porosity. For this purpose, tests were carried out using helium pycnometry on macro-agglomerated (8 % aromatic adhesive) and micro-agglomerated (20 % aromatic adhesive) cork bodies. These measurements give an open porosity of 1.8 % (v/v) for macro-agglomerated cork. However, the open porosity was not measurable with this technique in the case of micro-agglomerated cork. This means that micro-agglomerated cork is either nonporous or the porosity is not accessible to helium. This confirms the decrease in porosity observed by SEM when smaller cork particles are used. In macro-agglomerated cork, an important intergranular porosity is visible (Fig. 6a). By contrast, for micro-agglomerated cork, this porosity appears to be absent and the adhesive is obstructing the residual porosity between the cork particles (Fig. 6b), thus contributing to increase the barrier property of agglomerated cork.

3.2. Effect of compression

The CO_2 barrier properties of agglomerated cork bodies presented above were determined for non-compressed samples (Table 1). In fact, considering the oenological application, the stoppers are compressed in the bottleneck (17 mm diameter). This leads to a total volume reduction of 70 %, and can thus strongly impact the gas transfer. The effect of such a compression level on the CO_2 effective diffusion coefficient is reported in Fig. 7 for the macro- and micro-agglomerated corks.

There is a significant reduction in the effective diffusion coefficient for both macro- and micro-agglomerated corks when the agglomerated cork body is compressed. The effective diffusion coefficient value decreases by a factor of around 6000 for macro-agglomerated cork (from 3×10^{-5} to 5×10^{-9} $m^2.s^{-1}$) and by a factor of around 1000 for micro-agglomerated cork (from 8×10^{-8} to 8×10^{-11} $m^2.s^{-1}$) (Table 2). The level of compression, as applied in the bottleneck, therefore greatly reduces the transfer of gas through the agglomerated cork body. This improvement in barrier properties can be explained, in a large part, by the very high reduction in volume. By reducing the intergranular porosity and increasing the tortuosity, the compression slows down the diffusion processes of Darcy and Knudsen. This is particularly true for macro-agglomerated cork for which the intergranular porosity is larger than for micro-agglomerated cork. The decrease in the effective diffusion coefficient due to compression was 6 times larger than for micro-agglomerated cork. In addition, there is also a significant reduction in the width of the distribution, which means that the compression also makes the samples more homogeneous from the diffusion point of view.

3.3. Role of the cork discs

Previous investigations have clearly shown that the formulation parameters, as well as the compression, can strongly change the barrier properties of the agglomerated cork body. It

is also important to study the role that the two cork discs attached at one end of the cork body may play in the gas transfer through the sparkling wine stopper. The cork disc is punched in the plane perpendicular to the radial direction, and thus it is sprinkled with lenticels, which are channels oriented in a direction parallel to the gas flow. Permeation tests were carried out on single cork discs, but the gas flow is too fast for being measured with our manometric device. In this case and the CO_2 effective diffusion coefficient is taken equal to the value in air (Table 2). Thus, the cork disc alone is not an efficient barrier to the gas diffusion, at least when it is considered non-compressed.

Nevertheless, in the cork stopper, these cork discs are glued together with an aqueous dispersion of PUs. The effective diffusion coefficient of CO_2 was measured through a film of ~700 µm thickness of this adhesive. A mean value of 4×10^{-11} $m^2.s^{-1}$ was found (Table 2). In order to get closer to the industrial cork manufacturing process, the effective diffusion coefficient of CO_2 was also measured through the two cork discs glued together with a single film of adhesive in between (a sample of ~9 mm thickness was taken from the two discs at the end of a MA2D industrial stopper). In this case, the mean value is 6×10^{-13} $m^2.s^{-1}$ (Table 2). This is very surprising. Such a difference can be explained by the following reasons. i) As we consider no resistance to gas transfer in cork discs, this effective diffusion coefficient is calculated by taking a thickness of adhesive film of 10 µm, roughly estimated from SEM observation (Fig. 8). ii) During the industrial process, the adhesive layer is deposited in excess and can migrate into the lenticels, causing a local increase in the thickness of the adhesive film. iii) Polymerization under industrial conditions differs considerably from that applied under laboratory conditions to obtain a self-supporting film at 25°C. iv) Reactions occurring at the interface between cork and adhesive may locally create an additional barrier to gas transfer. These effects may also explain the large distribution of effective D values measured on this system (ranging from 9×10^{-14} to 3×10^{-12} $m^2.s^{-1}$).

Therefore, it appears that the adhesive film used to glue the two cork discs can act as a significant barrier to the CO_2 transfer, provided that the film is sufficiently thick and homogeneous.

3.4. Critical discussion of CO_2 transfer in a sparkling wine cork stopper

This work allows the determination of the effective diffusion coefficient values for the different parts composing a sparkling wine stopper as well as the formulation and processing parameters that can influence the gas transfer. For a deeper understanding, it is essential to couple these data together in order to elucidate the mechanisms involved in the gas diffusion when considering the material as a whole (Fig. 9).

Gas transfer through the agglomerated cork body

For the gas transfer through the cork body, the CO_2 effective diffusion coefficient for a non-compressed macro-agglomerated cork is about 3×10^{-5} $m^2.s^{-1}$. This very high value shows that the gas diffusion is very fast, probably because of an important intergranular porosity. As the CO_2 diffusion coefficient in air is 1.39×10^{-5} $m^2.s^{-1}$ (at 24 °C and 0.1 MPa)[20], it can be assumed that the porosity is totally open along the entire macro-agglomerated cork body. In such a case, the diffusion is mainly governed by Darcy's and Knudsen's mechanisms in the intergranular porosity, considering the very high value of D. This is reinforced by the fact that similar effective diffusion coefficients were obtained for O_2 on non-compressed macro-agglomerated cork body (data not shown). However, the solution-diffusion mechanism may also still be involved to cross the cork cell walls as well as the adhesive network at some points. For the micro-agglomerated cork, solution-diffusion process is probably the main mechanism involved and acting as the limiting step to gas transfer (even

303 if Darcy's and Knudsen's mechanisms occur), since the porosity is reduced, leading to a
304 lower CO_2 effective diffusion coefficient of around 10^{-8} $m^2.s^{-1}$ in non-compressed samples. In
305 this case, there is also a difference between O_2 and CO_2 effective diffusion coefficients,
306 indicating that the solution-diffusion process plays a more important role than in the macro-
307 agglomerated cork body (data not shown). In conclusion, the three mechanisms coexist
308 simultaneously and in parallel within the stoppers. On the one hand, the higher the
309 interconnected porosity, the greater the permeability will be governed by Darcy's and
310 Knudsen's mechanisms. On the other hand, the smaller the porosity, or the higher the
311 adhesive concentration, the more the permeability will be governed by the solution-diffusion
312 process, and therefore the gas transfer will be slowed down.

313

314 **Gas transfer through the cork discs and the adhesive film between them**

315 For the cork discs, Darcy's mechanism is obviously involved in the lenticels oriented
316 in the transfer direction. As above-mentioned, it is experimentally impossible to determine
317 such a high effective diffusion coefficient value with the manometric method. However,
318 considering the lenticels as macropores, it can reasonably be assumed that the effective
319 diffusion coefficient would be at least of the same order of magnitude as its molecular value
320 in air (~ 10^{-5} $m^2.s^{-1}$).

321 The adhesive film between the two cork discs acts as an efficient barrier to gas
322 transfer. The gas transfer through this film is controlled by a solution-diffusion mechanism.
323 As we know the values of the CO_2 effective diffusion coefficient in the adhesive film between
324 the cork discs ($D = 6 \times 10^{-13}$ $m^2.s^{-1}$), the surface area of the film S taken as the section of the
325 bottleneck (m^2) and the temperature T (K), the gas flow J ($mol.s^{-1}$) can be calculated as a
326 function of the film thickness L (m) with the following equation:

$$J = D \times S \times \frac{\Delta p \times \psi}{R \times T \times L} \qquad (2)$$

where ψ is determined from the CO_2 sorption isotherm and corresponds to the partition coefficient, defined as the ratio between the concentration of CO_2 sorbed on the material ($mol.m^{-3}$) and the concentration of CO_2 in the gas phase in contact with the film ($mol.m^{-3}$) at equilibrium. A value of 0.3 was experimentally determined from the sorption isotherms for the adhesive (Fig. 3).

The dependence of the gas flow on thickness is shown in Fig. 10. From this plot, a critical thickness (L_{crit}) was determined by applying the tangent method on the hyperbolic curve and a constant thickness (L_{cst}) was defined as the thickness value above which the variation in gas flow becomes less than 5 % for each additional micrometer. Above a L_{cst} of around 20 µm, the gain in barrier property remains very low. By contrast, the gas flow drastically increases for a thickness lower than the L_{crit} value (around 5 µm). In the latter case, each micrometer decrease leads to a 20 to 50 % increase in the gas flow. In addition, SEM observations were performed on a cross-section of the two glued cork discs (Fig. 8). The film separating the two cork discs could be distinguished. In the upper disc, a lenticel is partially obstructed by the adhesive. As the adhesive has been deposited in excess, the excess glue has been evacuated at the periphery of the cork disc or through the open lenticular channels, as previously mentioned. Moreover, the adhesive film does not display a homogeneous thickness. It is on average quite thin, around 10 µm thickness (Fig. 8b). It also appears up to three times thicker at some places (Fig. 8c). Furthermore, the average thickness of the film between the two discs lies between L_{crit} and L_{cst} values, as previously defined (Fig. 10), which means that this film globally represents an efficient barrier to gas transfer.

Global effective diffusion coefficient through the full cork stopper

The different parts of the sparkling wine stopper are disposed in series as displayed in Fig. 2. Nowadays, two different cork stoppers are mainly used in the market for sparkling wine. (i) stoppers composed of a macro-agglomerated body with two cork discs at one end (MA2D) and (ii) stoppers composed only of a micro-agglomerated cork body (MI). Considering their respective assembly, a global resistance to mass transfer R ($s.m^{-1}$) and a global effective diffusion coefficient D ($m^2.s^{-1}$), can be calculated for these two types of stoppers.

A rather complex case is that of the MA2D stopper, composed of a macro-agglomerated cork body of 36 mm, with two cork discs of 6 mm each and two adhesive films of 10 µm each, as shown in Fig. 1. The global resistance to gas transfer is therefore the sum of local resistances corresponding to each part of this stopper (Fig. 2). Unlike the MI stopper, which is considered a homogeneous system with a single effective diffusion coefficient, the MA2D stopper is heterogeneous with, for each part, a corresponding effective diffusion coefficient and a solubility for CO_2. Its global effective diffusion coefficient can therefore be determined according to the following equation:

$$\frac{L_{stopper}}{D_{stopper}\psi_{stopper}} = \sum_i \frac{L_i}{D_i\psi_i} \qquad (3)$$

The values calculated for the global effective diffusion coefficient of each stopper are shown in Table 3, with, for each part composing the stopper, the respective values of thickness, partition coefficient, effective diffusion coefficient and resistance.

In this calculation, the following assumptions have been made. i) The effective diffusion coefficient values used for these calculations are taken from Table 2. It is assumed that that the corresponding effective diffusion coefficient in the cork body is not significantly different for the considered thickness in the cork stopper (as shown in Fig. 4). ii) The D value on one adhesive layer between two cork discs was measured on a non-compressed system. It

375 may be different when compressed. In addition, for the cork disc alone, it was not possible to
376 measure the effective diffusion coefficient on a compressed disc because it breaks during
377 compression. iii) The compression brought by the muselet on the outer part of the stopper is
378 not taken into account. iv) For the cork disc, a partition coefficient of 1 is used as the transfer
379 follows Darcy's mechanism. A value of 0.9 is used for the stopper and 0.3 for the adhesive
380 (Fig. 3). v) The gas transfer that may occur at the cork/bottleneck interface is not considered
381 in this work.

382 From equation 3, the limiting step to the gas transfer is therefore associated with the
383 part having the strongest resistance to gas transfer (Fig. 2). In this case, this is the adhesive
384 films used to glue the two cork discs (Table 2). Assuming that these films have no defect and
385 have sufficient thickness over the entire disc surface, this is the essential part that is
386 responsible for the barrier properties of MA2D stoppers. The global effective diffusion
387 coefficient of MI stopper was also calculated considering a micro-agglomerated cork body of
388 48 mm. When considered as non-compressed materials, the global resistance to gas transfer is
389 higher for MA2D than for MI stoppers (Table 3).

390 However, when used in compressed conditions for sparkling wine conservation, the
391 global effective diffusion coefficient and resistance to mass transfer change. Let us consider a
392 stopper partially inserted in a bottleneck with a penetration depth of 24 mm inside the
393 bottleneck and 16 mm remaining non-compressed outside. The global effective diffusion
394 coefficient D and resistance R calculated in these conditions for the MA2D and MI stoppers
395 are reported in Table 3. Regarding the value obtained, when the stoppers are considered as
396 compressed in the bottleneck, MI stoppers have a resistance to mass transfer 3 times higher
397 than a MA2D stopper.

398 Liger-Belair *et al.* were the first to estimate a CO_2 effective diffusion coefficient
399 through MA2D cork stoppers for sparkling wine, based on the dissolved CO_2 concentration

decrease in different Champagne wine vintages (from 2 months to 35 years of storage)[5, 6]. However, they did not focus in detail on the transfer mechanisms acting in such a composite material. In the present work, the detailed study of the agglomerated cork stoppers allows us to clearly identify the limiting step to gas transfer and thus the parameters responsible for providing good barrier properties. The global effective diffusion coefficient value determined in our study is in the same order of magnitude (4×10^{-10} $m^2.s^{-1}$) as those reported by Liger-Belair *et al.* (from 5×10^{-11} to 3×10^{-10} $m^2.s^{-1}$) and measured in situ on different aged Champagne wine samples[5, 6]. The global effective diffusion coefficient calculated from the individual effective diffusion coefficients measured on each part is therefore in good agreement with the global effective diffusion coefficient values obtained from their *in situ* experiments.

Toward the shelf life prediction of corked bottles of sparkling wine based on CO_2 effective diffusion through the stopper

Bubble formation is indeed the hallmark of sparkling wines. The intensity of effervescence and the bubbles' size, two characteristics of paramount importance for sparkling wines lovers, both depend on the level of dissolved CO_2 found in a sparkling wine[21]. Nevertheless, below a critical level of dissolved CO_2 close to 2.5 $g.L^{-1}$ (at 12 °C), namely C_L^*, a sparkling wine becomes thermodynamically unable to promote any bubble formation under standard tasting conditions (i.e., in a glass, with micrometric particles or glass anfractuosities acting as bubble nucleation sites), as described by Liger-Belair[22]. The precise knowledge of the permeability of a cork stopper with regard to gas-phase CO_2 becomes therefore crucial to be able to understand how a sparkling wine will age as time proceeds, especially concerning its progressive decrease in dissolved CO_2. In bottles of sparkling wines sealed with cork stoppers, because the partial pressure of gas-phase CO_2 in the bottleneck reaches up to 6 bar (at 12 °C),

425 CO_2 slowly diffuses from the bottle to the ambient air, either through the cork bulk or through
426 the cork/bottleneck interface. By combining both Henry's and Fick's laws, an exponential
427 decay-type model was found for the theoretical time-dependent level of dissolved CO_2 found
428 in champagne during aging (in the MKS system of units)[5]:

429 $$\begin{cases} C_L(t) \approx C_0 \, exp\left(-\frac{t}{\tau}\right) \\ with \, \tau = \frac{L(V_G + k_H R T V_L)}{DS} \end{cases} \quad (4)$$

430 with C_0 the initial level of dissolved CO_2 after corking the bottle, t the aging period of time,
431 τ the timescale of the exponential decay-type model, L the total length of the cork, V_L the
432 volume of the liquid phase in the sealed bottle, k_H the temperature-dependent Henry's law
433 constant of CO_2 (conveniently expressed in $mol.m^{-3}.Pa^{-1}$)[22], V_G the volume of gas phase
434 (the headspace) in the sealed bottle, R the ideal gas constant (8.31 $J.K^{-1}.mol^{-1}$), T the
435 temperature, D the global diffusion coefficient of gas-phase CO_2 through the cork stopper,
436 and S the cross section of the cork stopper (equivalent indeed to the cross section of the
437 bottleneck). The global D values (given in Table 3) are used in this calculation.

438 Following the exponential decay-type law given by equation 4, it becomes therefore possible
439 to predict the shelf life of corked bottles of sparkling wines (i.e., the time beyond which the
440 concentration of dissolved CO_2 fall below the critical concentration of 2.5 $g.L^{-1}$ required for
441 bubbling)[6]. Replacing $C_L(t)$ in equation 4 by the critical concentration of dissolved CO_2
442 below which bubble formation would become impossible, and developing, leads to the critical
443 aging period of time, denoted t_B^*, beyond which bubbling would become impossible through
444 lack of dissolved CO_2:

445 $$t_B^* \approx \tau \ln\left(\frac{C_0}{C_L^*}\right) \quad (5)$$

By replacing in the latter equation each parameter by its numerical value, it becomes therefore possible to approach the maximum period of aging (and therefore a shelf life prediction) beyond which a bottle of sparkling wine could become flat. For a standard 75 cL bottle of sparkling wine initially holding a level of dissolved CO_2 close to 12 $g.L^{-1}$[21], the theoretical mean shelf life prediction is in the order of 10 years if the bottle is sealed with a MA2D cork stopper. The distribution is rather large, from 2 to 65 years, if we consider the minimum and maximum values for all the parts composing the stopper, and underlines the crucial barrier role of the adhesive film between the discs. If the same bottle of sparkling wine is sealed with a MI cork stopper, its theoretical mean shelf life prediction is increased to about 30 years. In this case, the distribution is reduced, ranging from 20 to 50 years. A shelf life prediction of 30 years before the sparkling wine would become flat is nevertheless quite hard to verify in situ, because MI cork stoppers have only been used for about two decades only. In contrast, MA2D cork stoppers have been used to seal bottles of champagne and sparkling wines for several decades. Time series data recordings of dissolved CO_2 were already done in situ with cuvees sealed with MA2D cork stoppers and aged from several years up to several decades[5, 6, 23]. The dissolved CO_2 content found in these bottles having aged for a much longer period of time than the theoretical shelf life prediction of 10 years was found to be still much higher than the critical level of 2.5 $g.L^{-1}$ required for bubble formation. Moreover, it is worth noting that the global diffusion coefficients determined under compressed conditions in the present work do not take into account the gas transfer that may occur at the cork/bottleneck interface[16, 24]. Taking this into account would even more increase the respective global diffusion coefficients, therefore leading to theoretical shelf life predictions even shorter. We are therefore strongly tempted to conclude that the real storage conditions experienced by the corks are in favor of a much better impermeability with regard to gas-phase CO_2. This is the

reason why Champagne and sparkling wine bottles can age for several decades before they lose their bubbling capacity.

A crucial point also finally unveiled by this work is that, the dry compressed conditions, under which global CO_2 diffusion coefficients have been determined in the present work, are still far from the real conditions found in a bottleneck. In a bottleneck, the cork ages in contact with the wine (if bottles are stored horizontally) or in contact with a vapor phase saturated with water and ethanol (if the bottles are stored vertically). Changes in the structure of the cork during aging could therefore alter the way in which CO_2 molecules move from the headspace of the bottle to the ambient air, either through the cork stopper, or through the interface between the bottleneck and the cork stopper. Moreover, it is possible that prolonged aging could progressively moisturize the cork stopper, thus filling the pores, and reducing in turn the global diffusion coefficient of CO_2 through the cork stopper. Further experiments are needed to fully understand how the global diffusion coefficient of CO_2 through cork stopper could change as time proceeds during aging.

4. Conclusion

This study clearly identified the parameters that can influence the gas barrier properties through sparkling wine cork stoppers. The parameter having the strongest impact on the barrier properties is the compression of the agglomerated cork body, which drastically reduces the effective diffusion coefficient, when applying a 70 % reduction in volume, corresponding to the compression in the bottleneck. Other parameters with a significant impact on the CO_2 effective diffusion are the cork particle size along with the adhesive concentration in the agglomerated cork body. The smaller the cork particles and, correlatively, the higher the adhesive concentration, the higher the CO_2 barrier property. Both of these associated

parameters result in a decrease of the intergranular porosity. Nevertheless, this effect tends to be mitigated when the samples are highly compressed.

The limiting step to gas transfer is the diffusion through the adhesive present both in the network of the agglomerated cork body and in the film between the two cork discs. The diffusion mechanism involved is thus the solution-diffusion process through the adhesive polymeric network. Given these results, it is therefore essential that the adhesive network, particularly that between the two cork discs, is as homogeneous as possible and sufficiently thick to act as an efficient barrier to gases.

Finally, it should be pointed out that the values reported in this study agree rather well with those obtained in real conditions of aging of Champagne wine, even if only the cork stopper is considered. Indeed, the role of the interface between the stopper and the bottleneck, and the surface treatment applied on the stopper were not taken into account. Moreover, the evolution of the mechanical and barrier properties during real bottle aging could also play an important role, in particular when considering the stopper in contact with an hydroethanolic solution. However, this study clearly shows the effectiveness of the cork stopper for the conservation of the sparkling wine and its ability to maintain a sufficient dissolved concentration and partial pressure of CO_2 in the headspace over many years.

ACKNOWLEDGMENT

We gratefully acknowledge Prats & Bonany, Relvas and the French Federation of Cork (FFL), as well as the French National Association of Research and Technology (ANRT) for their financial support. This work was also supported by the Regional Council of Bourgogne

Franche-Comté and the “Fonds Européens de DEveloppement Régional (FEDER). SEM images were performed at the Laboratoire Interdisciplinaire Carnot de Bourgogne with the help of Frédéric Herbst. We would also like to thank Frédéric Brand, from Louis Bouillot (Boisset company), for his kind help in using the industrial bottling machine for sample preparation.

REFERENCES

1. H. Pereira. Cork: Biology, production and uses. Elsevier: Amsterdam, The Netherlands, 2007.
2. U. Franken, H. Primke, C.D. Alvaro, Polyurethane hot-melt adhesives for the production of cork stoppers. 2001.
3. CETIE, Guide n°3. Bouchage de tirage et d'expédition pour vins mousseux de qualité produits dans des régions déterminées VMQPRD : sur bague couronne verre 29 et 26 mm NF H35-029 (2007).
4. M. Faiveley, Stratégies de fermentation appliquées aux boissons, Techniques de l'Ingénieur, F3550 (2009).
5. G. Liger-Belair, S. Villaume, Losses of dissolved CO_2 through the cork stopper during Champagne aging: toward a multiparameter modeling., Journal of Agricultural and Food Chemistry 59 (2011) 4051-4056.
6. G. Liger-Belair, D. Carvajal-Perez, C. Cilindre, J. Facque, M. Brevot, F. Litoux-Desrues, V. Chaperon, R. Geoffroy, Evidence for moderate losses of dissolved CO_2 during aging on lees of a champagne prestigue cuvee, Journal of Food Engineering 233 (2018) 40-48.
7. E.J. Waters, Z. Peng, K.F. Pocock, P.J. Williams, The role of corks in oxidative spoilage of white wines, Australian Journal of Grape and Wine Research 2 (1996) 191-197.
8. T. Karbowiak, R.D. Gougeon, J.B. Alinc, L. Brachais, F. Debeaufort, A. Voilley, D. Chassagne, Wine oxidation and the role of cork, Critical Reviews in Food Science and Nutrition 50 (2010) 20-52.
9. K. Crouvisier Urion, J.P. Bellat, R.D. Gougeon, T. Karbowiak, Gas transfer through wine closures: A critical review, Trends in Food Science and Technology 78 (2018) 255-269.
10. C. Brazinha, A.P. Fonseca, H. Pereira, O.M.N.D. Teodoro, J.G. Crespo, Gas transport through cork: Modelling gas permeation based on the morphology of a natural polymer material, Journal of Membrane Science 428 (2013) 52-62.
11. D. Rabiot, J. Sanchez, J.M. Aracil In *Study of the oxygen transfer trough synthetic corks for wine conservation*, Second European Congress of Chemical Engineering, Montpellier, Montpellier, 1999.
12. J. Sanchez, J.M. Aracil, Perméabilité gazeuse de différents obturateurs, Bulletin de l'OIV 71 (1998) 279-283.
13. Y. Vasserot, C. Jacopin, P. Jeandet, Effect of bottle capacity and bottle-cap permeability to oxygen on dimethylsulfide formation in Champagne wines during aging on the lees, American Journal of Enology and Viticulture 52 (2001) 54-55.
14. A. Lagorce-Tachon, T. Karbowiak, J.M. Simon, R. Gougeon, J.P. Bellat, Diffusion of oxygen through cork stopper: Is it a Knudsen or a Fickian mechanism?, Journal of Agricultural and Food Chemistry 62 (2014) 9180-9185.
15. J. Chanut, A. Lagorce, S. Lequin, R.D. Gougeon, J.M. Simon, J.P. Bellat, T. Karbowiak, Fast manometric method for determining the effective oxygen diffusion coefficient through wine stopper, Polymer Testing In Press (2020).
16. A. Lagorce-Tachon, T. Karbowiak, C. Paulin, J.M. Simon, R.D. Gougeon, J.P. Bellat, About the role of the bottleneck/cork interface on oxygen transfer, Journal of Agricultural and Food Chemistry 64 (2016).
17. G. Galland, T.M. Lam, Permeability and diffusion of gases in segmented polyurethanes: Structure-properties relations, Journal of Applied Polymer Science 50 (1993) 1041-1058.
18. L. Le Barbenchon, J. Girardot, J.-B. Kopp, P. Viot, Multi-scale foam: 3D structure:compressive behaviour relationship of agglomerated cork, Materialia 5 (2019) 100219.
19. J. Santamarina, G. Cho, Soil behaviour: The role of particle shape, Advances in geotechnical engineering : The Skempton conference (2004).
20. D. Pritchard, J. Currie, Diffusion of coefficients of carbon dioxide, nitrous oxide, ethylene and ethane in air and their measurement, European Journal of Soil Science 33 (1982) 175-184.
21. G. Liger-Belair, The physics behind the fizz in champagne and sparkling wines, The European Physical Journal Special Topics 201 (2012) 1-88.
22. G. Liger-Belair, Modeling the losses of dissolved CO_2 from laser-etched champagne glasses, Journal of Physical Chemistry B 120 (2016) 3724-3734.
23. G. Liger-Belair, Effervescence in champagne and sparkling wines: From grape harvest to bubble rise, The European Physical Journal Special Topics 226 (2017) 3-116.
24. T. Karbowiak, K. Crouvisier Urion, A. Lagorce, J. Ballester, A. Geoffroy, C. Roullier-Gall, J. Chanut, R.D. Gougeon, P. Schmitt-Kopplin, J.P. Bellat, Wine aging: A bottleneck story npj Science of Food 3 (2019) Article 14.

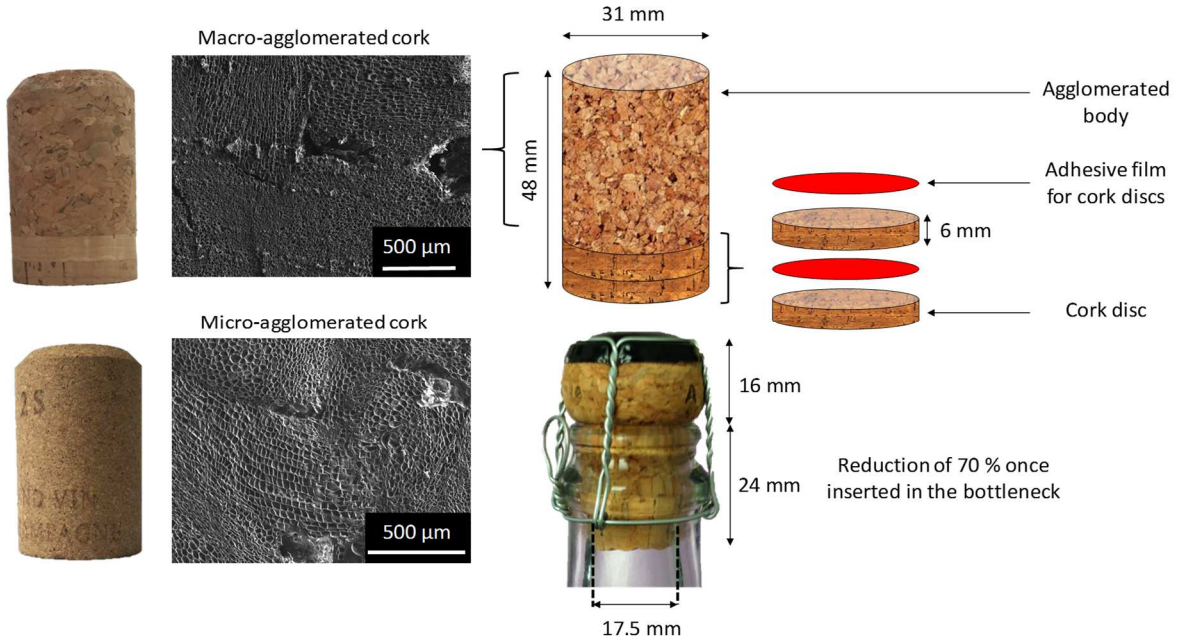

Fig. 1. Detailed structure of agglomerated cork stoppers used for sparkling wines, consisting of macro or micro cork particles, and usually two additional cork discs. The reduction in volume when the cork stopper is inserted into a bottleneck is also indicated.

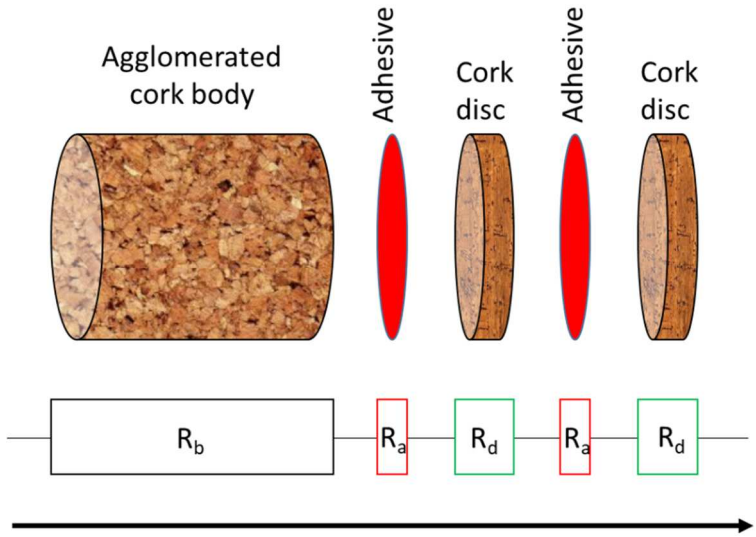

$$R_{stopper} = \sum_i R_i$$

$$\frac{L_{stopper}}{D_{stopper}\psi_{stopper}} = \sum_i \frac{L_i}{D_i\psi_i}$$

Fig. 2: The global resistance to mass transfer $R_{stopper}$ is the sum of local resistances R_i of each part of the sparkling wine stopper. The resistance to mass transfer (R) corresponds to the ratio of the thickness (L) to the effective diffusion coefficient (D) and the partition coefficient (ψ) of each part of the stopper the gas has to go through.

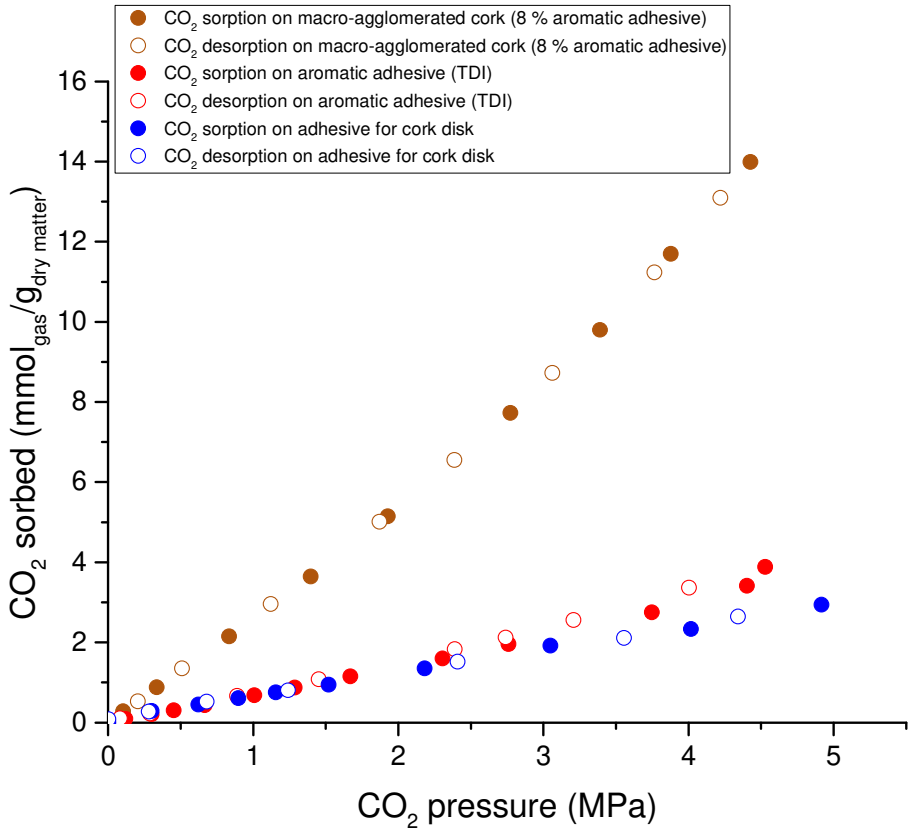

Fig. 3: Sorption-desorption isotherms of CO_2 on macro-agglomerated cork, aromatic adhesive and adhesive for cork disk, at 25 °C. The quantity of CO_2 sorbed is given in mmol of CO_2 per gram of dry matter.

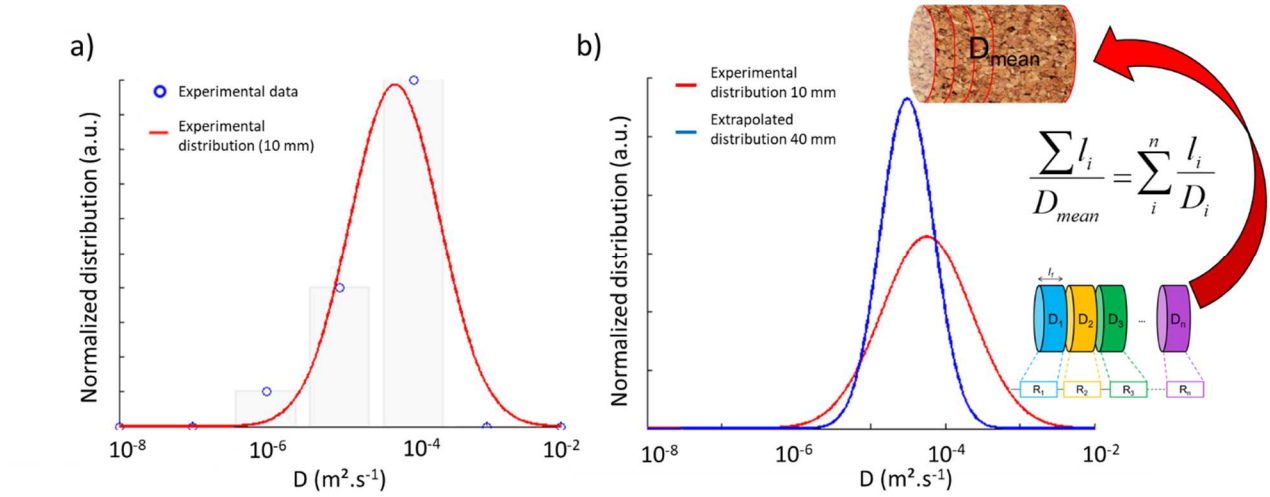

Fig. 4: a) Experimental data and normalized distribution obtained for the CO_2 effective diffusion coefficient values measured on 10 mm slices of macro-agglomerated cork body with 8 % of aromatic adhesive. b) Extrapolated distribution of the CO_2 diffusion coefficient (-) for a full-length stopper (40 mm) obtained from the experimental distribution (-) on 10 mm slices.

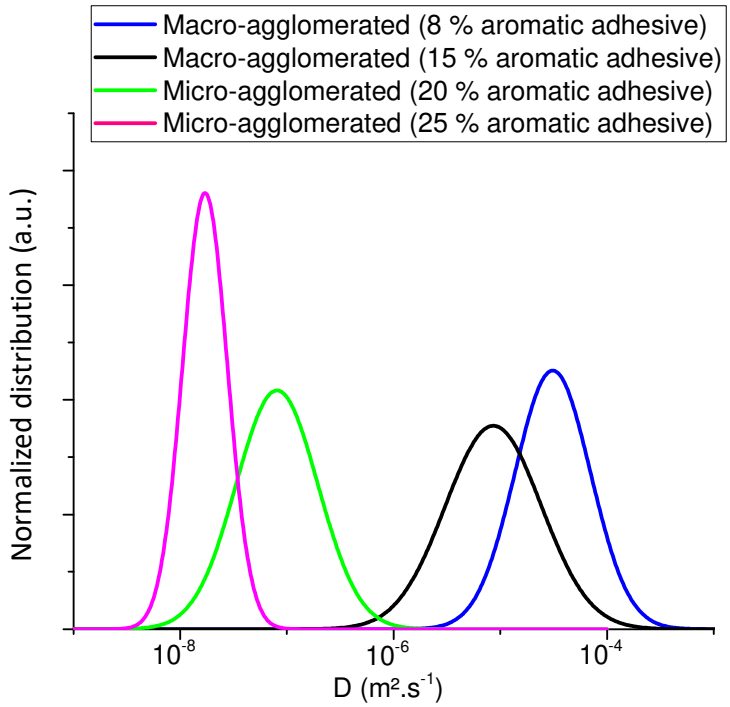

1

2 Fig. 5: Extrapolated distribution of CO_2 effective diffusion coefficients (D) through non-
3 compressed full-length (40 mm) macro-agglomerated cork body (with 8 % and 15 % m/m of
4 aromatic adhesive) and micro-agglomerated cork body (with 20 % and 25 % of aromatic
5 adhesive).

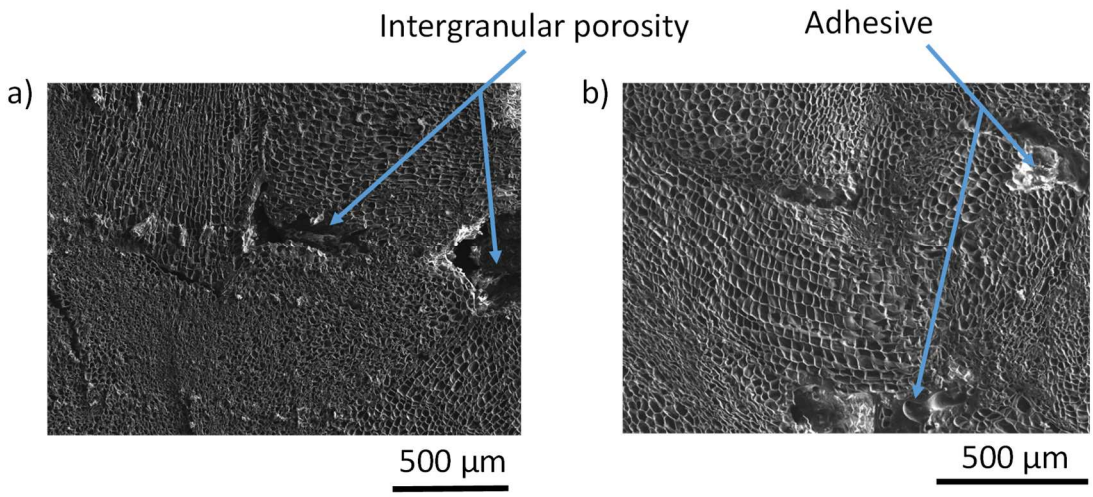

Fig. 6: SEM images of a) macro-agglomerated cork with intergranular porosity and b) micro-agglomerated cork with adhesive.

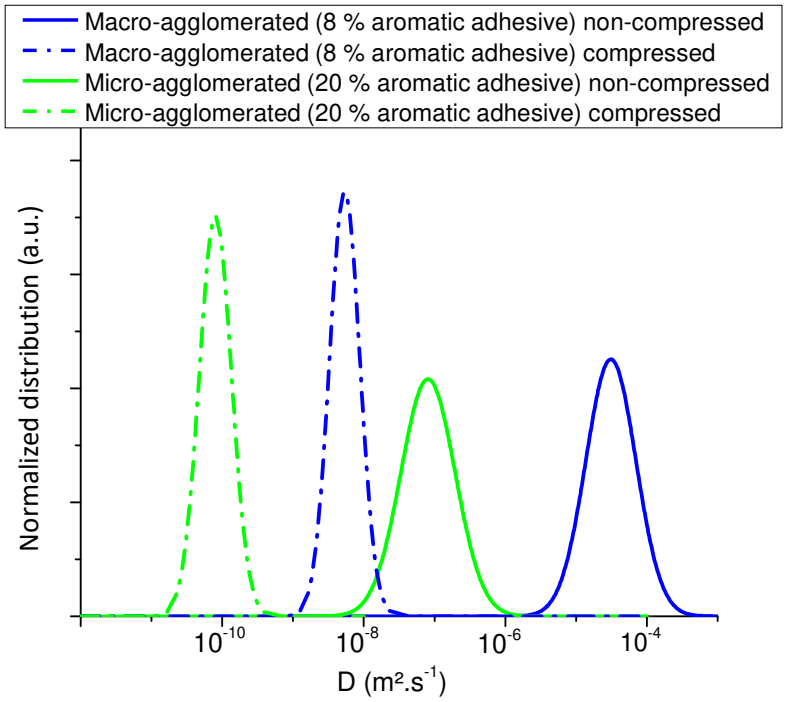

Fig. 7: Extrapolated distribution of CO_2 effective diffusion coefficient (D) through full-length (40 mm) macro-agglomerated cork body (with 8 % of aromatic adhesive) non-compressed (-) and compressed (- · -) and micro-agglomerated cork body (with 20 % of aromatic adhesive) non-compressed (-) and compressed (- · -). Sample diameters are reduced from 30 to 17 mm with the compression.

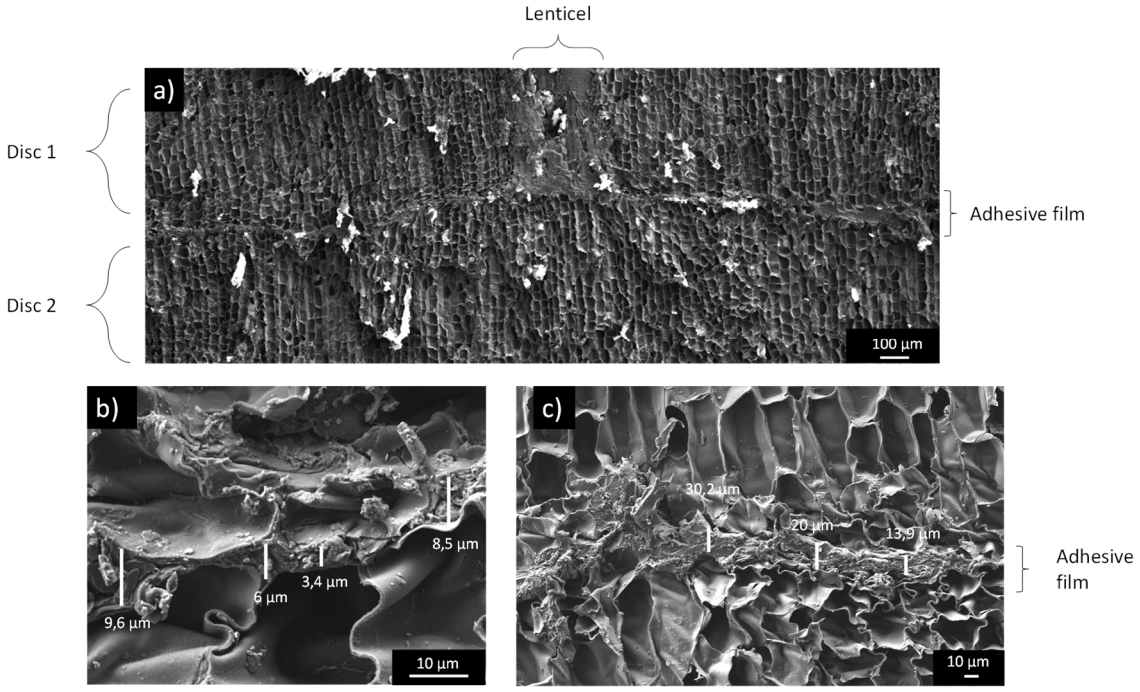

Fig. 8: SEM observations of: a) the adhesive film (aqueous dispersion of PUs) separating the two cork discs at the end of a sparkling wine stopper; b) and c) magnified selected film sections with indication of the thickness.

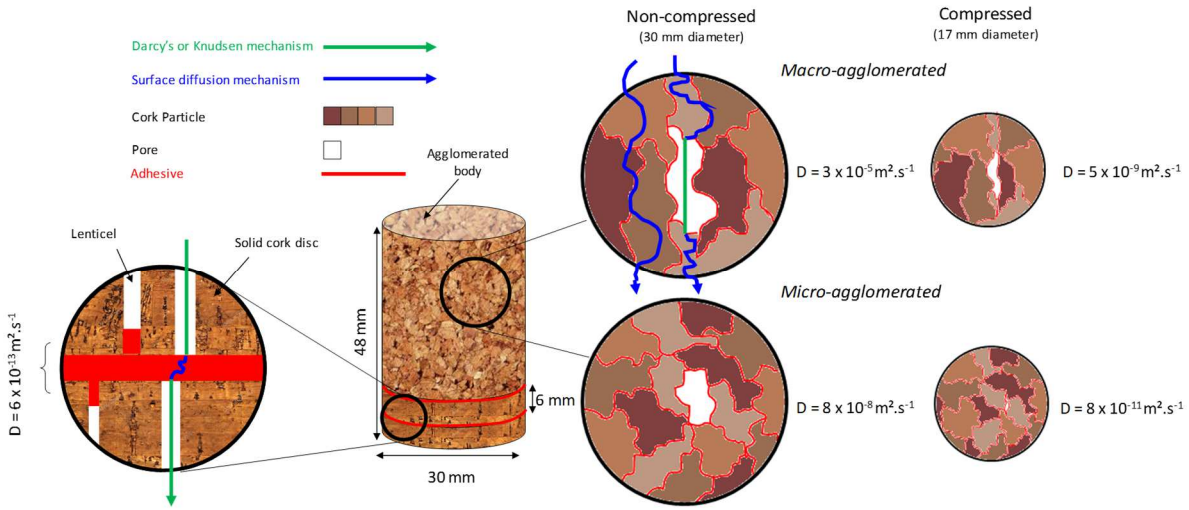

Fig. 9: Comprehensive overview of CO_2 effective diffusion coefficient values determined for the different parts comprising a cork stopper for sparkling wine and depiction of the mechanisms involved in the gas transfer. The diffusing mechanisms are only represented for the non-compressed macro-agglomerated cork, but occur in a similar manner in the micro-agglomerated cork and the compressed samples.

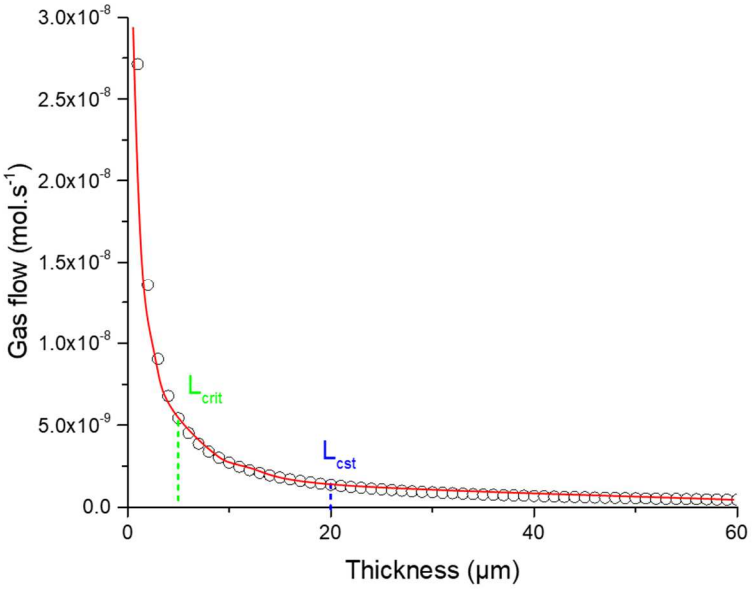

Fig. 10: Effect of the film thickness on the CO_2 flow through the adhesive film used between the two cork discs. The gas flow was calculated from the Equation 2 for a film thickness from 1 to 60 µm (each point corresponds to 1 µm).

Table 1: Sample geometry and conditions used to determine the effective diffusion coefficient of CO_2 in the different parts composing the sparkling wine stopper.

Sample part	Geometry	Extrapolated length	Number of replicates
Agglomerated cork body Non-compressed	Slice of 10 mm thickness Diameter: 30 mm	40 mm	15
Agglomerated cork body Compressed	Slice of 6 mm thickness Diameter: 17 mm	40 mm	10
Adhesive for agglomerated body Non-compressed	Film of ~700 µm thickness	-	10
Adhesive for cork discs Non-compressed	Film of ~700 µm thickness	-	10
Two cork discs with the adhesive layer in between Non-compressed	Slice of 9 mm thickness Diameter: 30 mm	-	15

Table 2: Mean values of CO_2 effective diffusion coefficient, D ($m^2.s^{-1}$), at 25 °C, obtained from the extrapolated distribution to 40 mm length for the agglomerated cork samples or from the experimental distribution for the adhesive film samples. Data in brackets are minimum and maximum values including standard deviation from the corresponding distribution. (n.d.: not determined)

Sample	Mean D ($m^2.s^{-1}$) *(Dmin - Dmax)*
Macro-agglomerated 8 % aromatic non-compressed cork body	3×10^{-5} *($1 \times 10^{-5} – 7 \times 10^{-5}$)*
Macro-agglomerated 15 % aromatic non-compressed cork body	9×10^{-6} *($3 \times 10^{-6} – 2 \times 10^{-5}$)*
Micro-agglomerated 20 % aromatic non-compressed cork body	8×10^{-8} *($3 \times 10^{-8} – 2 \times 10^{-7}$)*
Micro-agglomerated 25 % aromatic non-compressed cork body	2×10^{-8} *($1 \times 10^{-8} – 3 \times 10^{-8}$)*
Macro-agglomerated 8 % aromatic compressed cork body	5×10^{-9} *($3 \times 10^{-9} – 9 \times 10^{-9}$)*
Micro-agglomerated 20 % aromatic compressed cork body	8×10^{-11} *($5 \times 10^{-11} – 1 \times 10^{-10}$)*
Aromatic adhesive for cork body (film of ~700 µm thickness)	8×10^{-11} *($2 \times 10^{-11} – 3 \times 10^{-10}$)*
Adhesive for cork disc (film of ~700 µm thickness)	4×10^{-11} *($2 \times 10^{-11} – 9 \times 10^{-11}$)*
Cork disc	n.d. ≈ D CO_2 in air (≈ 10^{-5})
One adhesive layer in between two cork discs, non-compressed (film of 10 µm estimated thickness, based on SEM pictures)	6×10^{-13} *($9 \times 10^{-14} – 3 \times 10^{-12}$)*

Table 3: Values of the global effective diffusion coefficient D ($m^2.s^{-1}$) calculated from the mean effective diffusion coefficient of the different individual parts, their partitioning coefficient for CO_2 and their respective thickness L (m), considering various assembly geometries. The global D value (given in bold for each case) was calculated assuming the global resistance to mass transfer as the sum of the resistances of all stopper parts.

Stopper	**Stopper part**	**Thickness L ($\times 10^{-3}$ m)**	**Partitioning coefficient ψ**	**Effective diffusion coefficient D ($m^2.s^{-1}$)**	**Resistance R ($s.m^{-1}$)**
	Non-compressed macro-agglomerated cork body	36	0.9	3×10^{-5}	1×10^{3}
	Adhesive layer (x2) *	0.01	0.3	6×10^{-13}	6×10^{7}
	Cork disc (x2) **	6	1	1×10^{-5}	6×10^{2}
MA2D non-compressed		**48**	**0.9**	**4×10^{-10}**	**1×10^{8}**
	Non-compressed micro-agglomerated cork body	48	0.9	8×10^{-8}	7×10^{5}
MI non-compressed		**48**	**0.9**	**8×10^{-8}**	**7×10^{5}**
	Non-compressed macro-agglomerated cork body	16	0.9	3×10^{-5}	6×10^{2}
	Compressed macro-agglomerated cork body	12	0.9	5×10^{-9}	2×10^{6}
	Adhesive layer (x2) *	0.01	0.3	6×10^{-13}	6×10^{7}
	Cork disc (x2) **	6	0.3	1×10^{-5}	6×10^{2}
MA2D inserted in bottleneck**		**40**	**0.9**	**4×10^{-10}**	**1×10^{8}**
	Non-compressed micro-agglomerated cork body	16	0.9	8×10^{-8}	2×10^{5}

	Compressed micro-agglomerated cork body	24	0.9	8×10^{-11}	3×10^{8}
MI inserted in bottleneck* **		**40**	**0.9**	**1×10^{-10}**	**3×10^{8}**

*Value measured on one adhesive layer between two cork discs, non-compressed

** Value taken as D CO_2 in air

** The gas transfer that may occur at the cork/bottleneck interface was not considered in this work (The bottleneck is only used for illustration purpose of the corresponding case study)

Graphical abstract